ELSEVIER

www.elsevier.nl/locate/carres

Carbohydrate Research 321 (1999) 88–95

CARBOHYDRATE RESEARCH

Solution conformation and dynamics of the trisaccharide fragments of the O-antigen of *Vibrio cholerae* O1, serotypes Inaba and Ogawa

Leandro González [a], Juan Luis Asensio [a], Alina Ariosa-Alvarez [b], Vicente Vérez-Bencomo [b], Jesús Jiménez-Barbero [a,*]

[a] *Departamento Química Orgánica Biológica, Instituto Química Orgánica, CSIC, Juan de la Cierva 3, E-28006 Madrid, Spain*

[b] *Laboratorio de Antigenos Sinteticos, Facultad de Quimica, Universidad de la Habana, Ciudad de la Habana 10400, Cuba*

Received 12 March 1999; accepted 19 June 1999

Abstract

The conformational behavior of the trisaccharide fragments of the Ogawa and Inaba *Vibrio cholera* serotypes has been studied using NMR and molecular dynamics (MD). The obtained results indicate that there are no significant differences in the major conformation and in the extent of motion of the glycosidic torsions of these molecules. The differences in biological activity are probably not due to conformational effects but to van der Waals and/or hydrogen bonding interactions between the antigens and the biological receptor. © 1999 Elsevier Science Ltd. All rights reserved.

Keywords: *Vibrio cholera*; Serotypes; NMR spectroscopy; Molecular mechanics

1. Introduction

The most common pathogen causing epidemic cholera is *Vibrio cholera* of serogroup O1 [1–4]. Ogawa and Inaba are the serotypes that constitute specific antigens [1–4]. Both structures are immunologically recognized with a high degree of crossreactivity, but also in a serotype-specific fashion. The specific recognition was expected to be associated with a short fragment at the 'nonreducing' end of the polysaccharides because the only difference between the serotypes is the presence in the Ogawa O-polysaccharide portion (O-PS) of an O-2 methylation in the terminal 'nonreducing' sugar. Moreover, it was demonstrated with polyclonal [5] and monoclonal [6] antibodies that the terminal mono- and disaccharides are responsible for the Ogawa specific recognition.

An understanding of the O-PS mode of binding by IgG antibodies and the three-dimensional structures of the bound antigen would be of major importance in the design of an efficient vaccine against cholera. The serotype-specificity of the *V. cholerae* resides in the O-PS of the lipopolysaccharides, which is located in the outer membrane of such pathogens. The O-PSs of Ogawa and Inaba are composed of a chain of 15 α-(1→2)-linked D-perosamines with their amino groups acylated with 3-deoxy-L-*glycero*-tetronic acid [1–

* Corresponding author. Tel.: +34-91-562-2900; fax: +34-91-564-4853.

0008-6215/99/$ - see front matter © 1999 Elsevier Science Ltd. All rights reserved.
PII: S0008-6215(99)00167-6

4]. The only difference between both serotypes is the presence of O-2 methylation in the terminal nonreducing sugar of the Ogawa serotype [1–4]. In addition, different results have demonstrated that the absolute configuration of the perosamine residue plays a key role in the expression of the serological specificity of the Inaba antigen factor C of *V. cholerae* O1 [7].

From an immunological point of view, the understanding of the mode of binding of the O-PS to IgG antibodies is of major importance. In this process, knowledge of the 3D structure of the bound antigen would be vital [8,9]. The first step of this study requires knowledge of the spatial structure and dynamics of the antigen in the free state. Since Ogawa and Inaba serotypes are linear homopolysaccharides, which only differ in the O-2 methylated terminal nonreducing sugar, knowledge of the conformational behavior and of the extent of motion of the glycosidic angle torsions in the minimum biologically active trisaccharide fragments of the antigens [10] may be used as a model to understand the behavior of the O-PS in the free state.

2. Materials and methods

Molecular mechanics and dynamics calculations.—The torsional angles ϕ and ψ are defined as H-1 C-C-1 C-O-1 C-C-2 B and C-1 C-O-1 C-C-2 B-H-2 B, for the linkage between the nonreducing end and the second residue and H-1 B-C-1 B-O-1 B-C-2 A and C-1 B-O-1 B-C-2 A-H-2 A, for the linkage between the second residue and the reducing end. The 3-deoxy-L-*glycero*-tetronic acid chain is indicated by Greek letters.

Molecular mechanics (MM) and molecular dynamics (MD) calculations and simulations were performed using the MM3* force field [11], as integrated in MACROMODEL [12]. First, potential-energy maps were calculated for the constituent disaccharide fragments: relaxed (Φ, Ψ) potential-energy maps were calculated as described [13]. One initial geometry of the secondary hydroxyl groups of the pyranoid moieties was considered, r (reverse clockwise). The previous step involved the generation of the corresponding rigid residue maps by using a grid step of 18°. Then, every Φ, Ψ point of this map was optimized using 200 steepest descent steps, followed by 1000 conjugate gradient iterations. From these relaxed maps, the probability distributions were calculated for each ϕ, ψ according to a Boltzmann function at 303 K.

The starting structures of both trisaccharides **1** and **2** of the polysaccharide were built by combining the more stable conformers (A and B) of the two glycosidic linkages and subjecting them to extensive energy minimization with conjugate gradients (maximum derivative < 0.001 kcal/Å). An extended structure of the acyl chain was considered. These were then used as the starting geometries for MD simulations [14] at 300 K. The average temperature in the simulations was 300 K with S.D. ± 5 K. The GB/SA (generalized Born solvent-accessible surface area) solvent model for water [15] was used for the MM3* simulations with a time step of 1 fs. The equilibration period was 100 ps. After this period, structures were saved every 0.5 ps. The total simulation time was 5 ns for every run. Four runs (with two initial conformers for each glycosidic linkage: AA, AB, BA, and BB) were performed. Similar results were obtained in all cases and then average distances between intra- and inter-residue proton pairs were calculated from the dynamic simulations.

The calculations were performed in a Silicon Graphics O2 workstation.

NMR spectroscopy.—NMR experiments were recorded on a Varian Unity 500 spectrometer, using approximately 3 mg/mL solution of the trisaccharides at different temperatures. Chemical shifts are reported in ppm using acetone as the internal reference (δ 2.225 ppm for ^{1}H and 30.5 ppm for ^{13}C). The double quantum filtered COSY spectrum was performed with a data matrix of 256×1K to digitize a spectral width of 2000 Hz; 16 scans were used with a relaxation delay of 1 s. The 2D TOCSY experiment was performed using a data matrix of 256×2K to digitize a spectral width of 2000 Hz; four scans were used per increment with a relaxation delay of 2 s. MLEV 17 was used for the 100 ms isotropic

mixing time. The one-bond proton–carbon correlation experiment was collected using the gradient-enhanced HMQC sequence. A data matrix of $128 \times 1K$ was used to digitize a spectral width of 2000 Hz in F_2 and 10,000 Hz in F_1. Four scans were used per increment with a relaxation delay of 1 s and a delay corresponding to a J value of 145 Hz. ^{13}C decoupling was achieved by the WALTZ scheme. The 2D-HMQC-TOCSY experiment was conducted with 80 ms of mixing time (MLEV 17). The same conditions as for the HMQC were employed. HMBC experiments were performed using the gradient-enhanced sequence with a data matrix of $256 \times 2K$ to digitize a spectral width of $2000 \times 15{,}000$ Hz; eight scans were acquired per increment with a delay of 65 ms for evolution of long-range couplings.

2D NOESY, 2D-ROESY, and 2D-T-ROESY experiments were performed using four different mixing times, namely 150, 300, 450, and 600 ms, with $256 \times 2K$ matrixes. Good linearity was observed up to 200 ms (NOESY) and 300 ms (ROESY). Estimated errors in the NOE intensities are $< 20\%$.

NOE calculations.—NOESY spectra were simulated according to a complete relaxation matrix approach following the protocol described previously [16], using four different mixing times (between 150 and 600 ms). The spectra were simulated from the average distances $\langle r^{-6} \rangle_{kl}$ calculated from the MD simulations. An isotropic motion and an external relaxation of 0.1/s were assumed. A τ_c of 175 ps was used to obtained the best match between experimental and calculated NOEs for the intra-residue proton pairs (H-1/H-2 for all residues). All the NOE calculations were performed automatically by a homemade program, available from the authors upon request [16].

3. Results and discussion

Conformational analysis: molecular dynamics studies.—In order to determine the overall 3D structure of the trisaccharides, molecular mechanics and dynamics calculations were performed. Information on the amount of conformational space accessible was obtained through MD simulations of **1** and **2** (Fig. 1). Simulations with the MM3* program and the GB/SA solvent model were performed as they have provided satisfactory results in the study of the conformation of a variety of oligosaccharide molecules [17]. First, relaxed potential-energy maps (Φ/Ψ) were calculated for the disaccharide fragment. The glycosidic linkage presents well-defined low-energy regions, with two major conformers, A and B, and a minor one, C, which covers $< 20\%$ of the complete potential-energy surface. The low-energy region (A and B conformers) show Φ values (Table 1) which are centered around those expected for the exo-anomeric effect [18], although the expected probability distributions occupy a wide surface. The associated relevant proton–proton inter-residue distances of the different maps that may be correlated

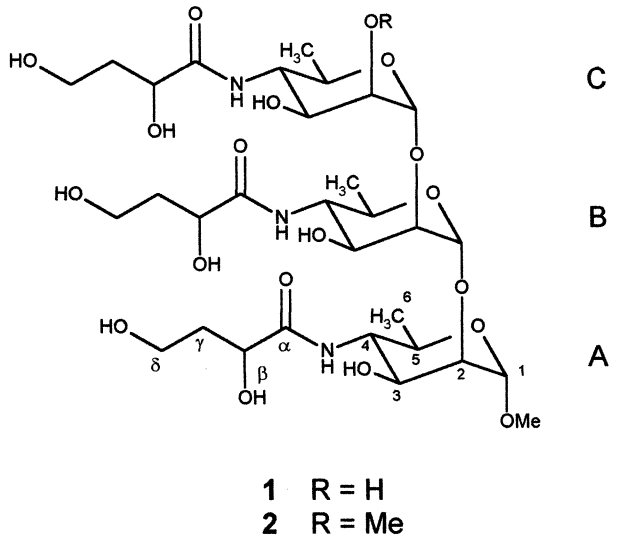

Fig. 1. Schematic view of compounds **1** and **2** showing the atomic numbering.

Table 1
Glycosidic torsion angle values (Φ, Ψ) of the predicted minima and MM3* populations (GB/SA solvent model) of the low-energy regions of trisaccharides **1** and **2** [a]

	Conformer		
	A	B	C
Torsion angle (Φ/Ψ)	−52/−25	−44/31	49/47
Population (%)	80.9	19.0	0.1

[a] The regions around Φ extend ca. 25 and 35° around Ψ. The results are basically identical for both compounds and both glycosidic linkages.

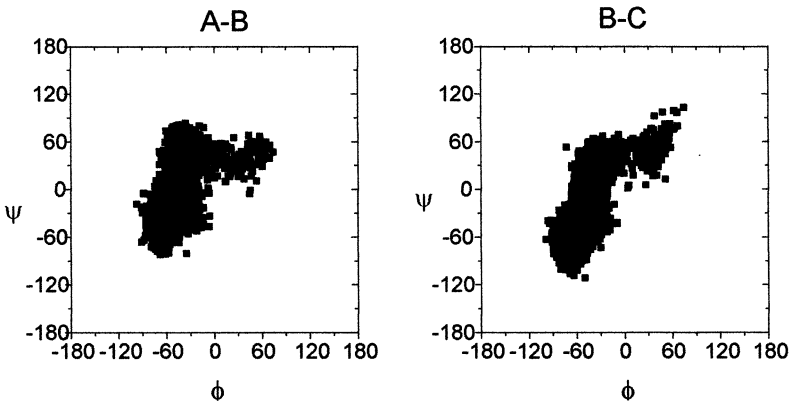

Fig. 2. Trajectory plots of the MD simulation (5 ns) of **1** by using MM3*. The trajectories of the simulation in Φ/Ψ space for every glycosidic linkage are shown.

with experimental NOE information [19] are similar to both glycosidic linkages, and therefore only one of them is given: short H-1 A–H-1 B and H-2 A–H-2 B distances are exclusive for conformer C. Short H-1 A–H-5 B and H-1 B–H-2 A distances are expected for both conformers A (2.3 and 2.6 Å, respectively) and B (3.1 and 2.3 Å, respectively), while a relatively short H-5 B–H-2 A distance (3.0 Å) corresponds with conformer A. Two models of trisaccharides **1** and **2** were then built, composed of the two glycosidic linkages of the molecule and the glycerotetronic acid chain, and submitted to different 5 ns simulations. For all linkages, the glycosidic torsion angles cover a well-defined part of the complete Φ/Ψ map (Fig. 2). The glycosidic torsion angles Φ and Ψ show oscillations centered at the regions of conformers A and B, although minor excursions to the region of conformer C are also observed. In all cases, these torsional oscillations are more pronounced around Ψ, as expected by the operativity of the exo-anomeric effect around Φ. No excursions to the anti Φ or Ψ regions were evident. In terms of the available space for the interglycosidic torsion angles, the calculated results are fairly similar for the α-(1→2) linkages, independent of the O-methyl substitution at the nonreducing end of the Ogawa serotype **2**. With respect to the accessible conformational space for the tetronic acid linkage, the results indicate a large accessible area of conformational space. In most cases, several transitions between the rotamers of the acid chain were observed. Nevertheless, it displayed either the *gg* or the *gt* conformations for most of the simulation time (>90%, [20]) Finally, the average expected interproton distances from the different MD simulations (Table 2) were estimated and compared to those observed experimentally. No close proton–proton distances were deduced from the MD models (Fig. 3), which were not apparent in the experimental NOE data.

A superimposition of different conformers found in the MD simulation is shown in Fig. 4. Despite the relatively narrow variation of the glycosidic torsion angles, the conformational space accessible to the tetronic acid chain may be large. Regarding the orientation of this chain, it may display a variety of orientations with respect to the sugar residues.

Table 2
Average relevant proton–proton inter-residue distances (Å) from the MD simulations for **1** and **2** and experimentally deduced NOE distances [a]

	MD	NMR
B H-1/A H-2	2.4	2.4–2.6
C H-1/B H-2	2.4	2.4–2.6
A H-1/B H-5	2.8	2.6–2.8
B H-1/C H-5	2.8	2.6–2.8
A H-2/B H-5	3.6	>3.5
B H-2/C H-5	3.6	>3.5
A H-1/B H-1	3.8	>3.5
B H-1/C H-1	3.8	>3.5
A H-2/B H-2	4.4	>3.5
B H-2/C H-2	4.4	>3.5
A H-1/A H-2	2.5	2.5
B H-1/B H-2	2.5	2.5
C H-1/C H-2	2.5	2.5

[a] The average simulation results for both compounds are basically identical. The values are rounded. Values >3.5 Å correspond to NOEs that were not observed.

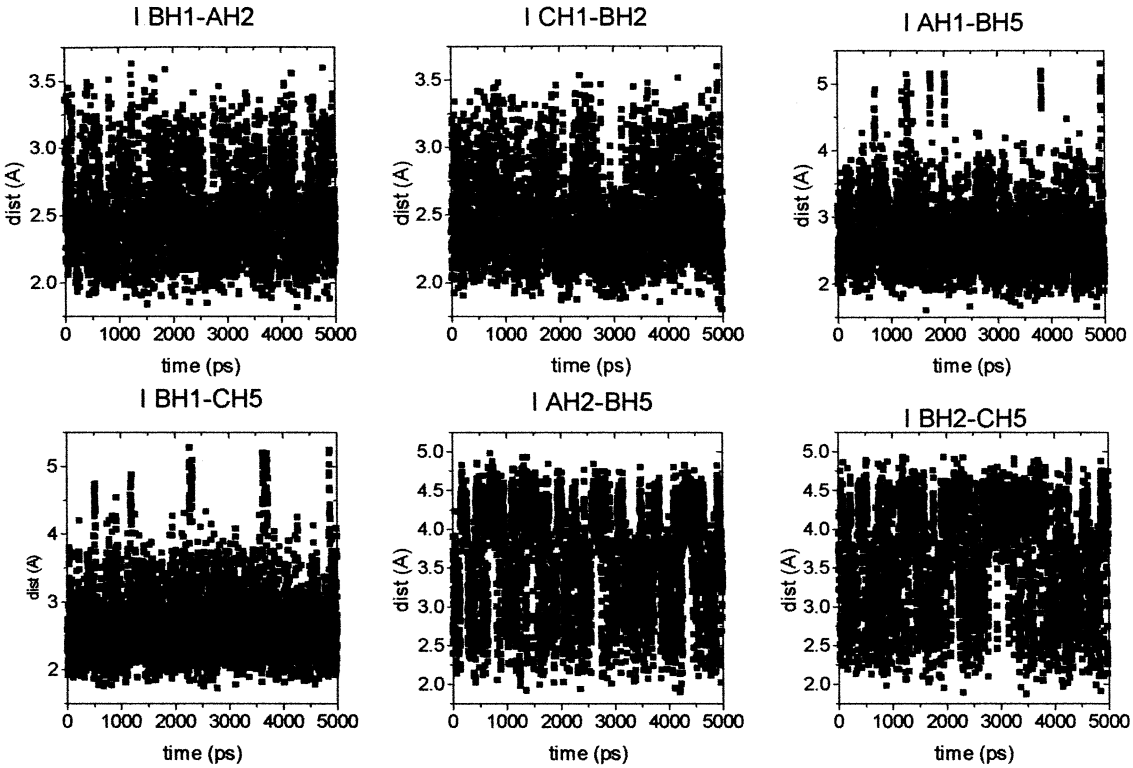

Fig. 3. History plots of the relevant proton–proton inter-residue distances across the different glycosidic linkages as calculated by one MD simulation (5 ns) of **1** using MM3*.

Nevertheless, a systematic calculation of the variation of the corresponding torsion angle indicates a preferred conformation around the C β–C γ linkages, with values of ca. 180° for (C α–C β–C γ–C δ), in agreement with the published X-ray structures [21,22] of the corresponding 2-OH and 2-OMe monosaccharides.

Similar results are observed for both trisaccharides **1** and **2**, regarding the oligosaccharide backbone and the lateral chain. Thus, the results do not depend on the nature of the O-methyl substitution acyl chain. Only a large variation on the orientation of the O-methyl chain was observed. A superimposition of different conformers found in the MD simulation is shown in Fig. 4.

^1H NMR.—Since NMR parameters are essentially time-averaged, it is possible to deduce the information from these experiments that corresponds to the time-averaged conformation in solution. The validity of the theoretical results has been tested using NMR measurements of vicinal coupling constants and NOEs. ^1H and ^{13}C NMR spectra were assigned completely by a combination of homonuclear COSY, TOCSY, and heteronuclear HMQC (Fig. 5), HMBC, and HMQC-TOCSY techniques. These latter two techniques were crucial for resolving the final ambiguities. The corresponding ^1H and ^{13}C NMR chemical shifts are listed in Table 3. No severe overlapping was observed and unambiguous conclusions could be obtained. For both oligosaccharides, the pyranoid rings can be described as essentially monoconformational $^4C_1$, as deduced from the vicinal pro-

Fig. 4. Superimposition of different snapshots of the Ogawa trisaccharide taken from MD simulations. The existence of an important amount of flexibility around the glycosidic linkages is evident.

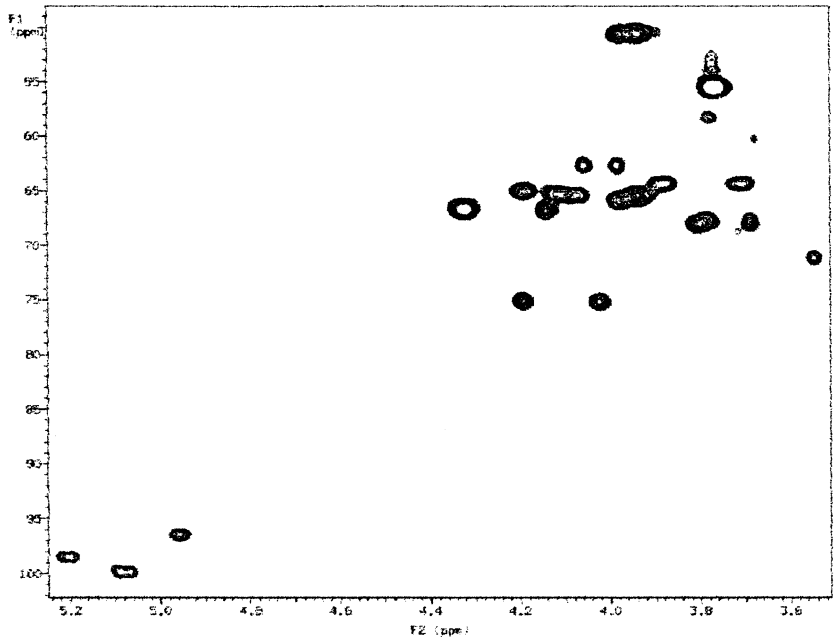

Fig. 5. Key regions of the HMQC 500 MHz spectra (mixing time 500 ms) at 299 K in D_2O.

ton–proton couplings (data not shown). NOESY and ROESY experiments were then used to qualitatively estimate proton–proton inter-residue distances [23]. For **1**, all NOESY cross peaks were positive (Fig. 6) at 500 MHz and 299 K. The distances were estimated using the isolated spin pair approximation and are given in Table 2. The H-1/H-2 intra-residue signals were used as a reference. The MD-calculated distances are also shown in Table 2. A satisfactory matching is observed between the distances found experimentally and those estimated through MD simulations, indicating a conformational equilibrium between A and B conformers. It is evident that conformer C is basically absent from the equilibrium, since no inter-residue H-1 C→H-1 B or H-2 C→H-2 B cross peaks could be detected. The inter-residue H-1 C–H-2 B (2.5 Å) and H-1 B–H-5 C (2.7 Å) distances are basically identical for both linkages and are in good agreement with the MD simulations. These experimental distances are in between those expected for conformers A and B (see above). On the other hand, no NOEs were observed for the H-2 C–H-5 B distance (exclusive for conformer A) as also deduced from MD simulations (average 3.5 Å).

The conformation of acetamido, formamido and amino derivatives of α-(1→2)-linked disaccharides has been studied previously [24]. These sugars appear in the structure of *Yersinia* O:9 and *Brucella abortus* polysaccharides and only differ in the carboxylic acid that acylates the amino group of the sugar. Indeed, some serological testing was performed to compare the *B. abortus* and *V. cholerae* cross-reactivity [25]. The only slight difference in conformational terms between those studies and these presented herein refer

Table 3
^1H and ^{13}C NMR chemicals (δ, ppm) shifts of methyl 4,6-dideoxy-4-(3-deoxy-L-*glycero*-tetronamido)-α-D-mannopyranosyl-(1→2)-4,6-dideoxy-4-(3-deoxy-L-*glycero*-tetronamido)-α-D-mannopyranosyl-(1→2)-4,6-dideoxy-4-(3-deoxy-L-*glycero*-tetronamido)-α-D-mannopyranoside (Inaba, **1**) in D_2O at 37 °C [a]

^1H	A	B	C	^{13}C	A	B	C
H(C-1)	4.88	5.13	5.00	C-1	99.2	101.2	102.4
H(C-2)	3.96	4.11	4.07	C-2	77.7	77.7	69.2
H(C-3)	4.00	3.91	3.87	C-3	68.2	68.5	68.2
H(C-4)	3.92	3.88	3.86	C-4	52.7	52.7	52.7
H(C-5)	3.84	3.91	3.87	C-5	66.7	67.2	66.7
H(C-6)	1.12	1.15	1.15	C-6	19.1	19.1	19.1
OMe	3.64				60.2		

[a] L-*glycero*-Tetronic acid: ($^1H/^{13}C$), α (C=O) 176.7 ppm, β 4.25/69.2 ppm, γ 1.81, 1.98/36.7 ppm, δ 3.73/58.2 ppm. The only differences for (**2**, Ogawa) are at position 2 of residue C (3.74/82.9 ppm) and OMe 3.46/62.7 ppm.

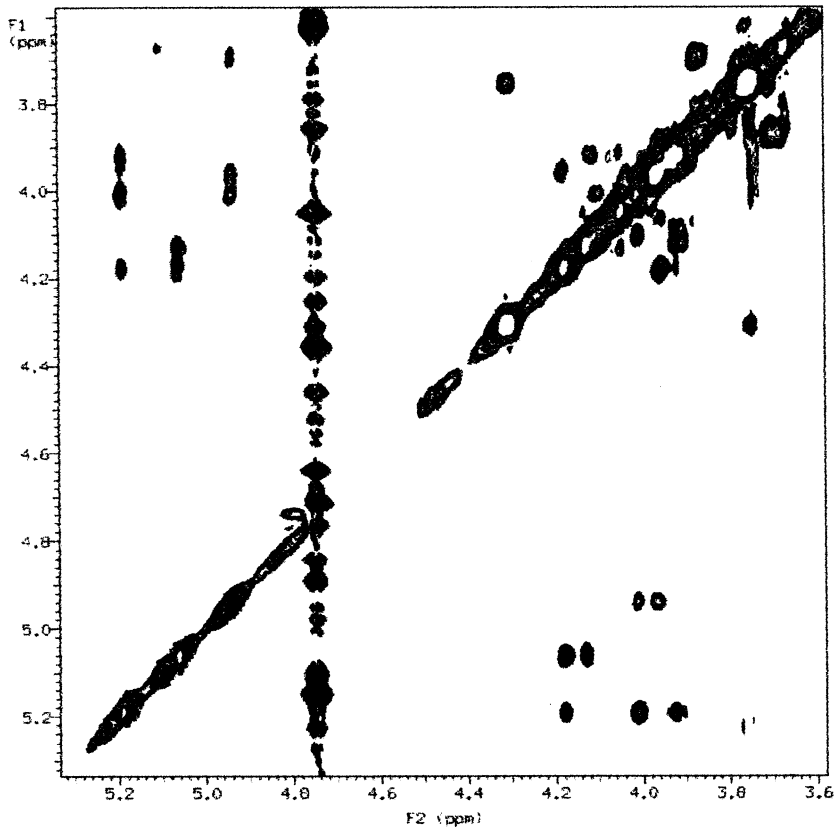

Fig. 6. Key regions of the NOESY 500 MHz spectra (mixing time 450 ms) at 299 K in D_2O.

to a slight change in the conformational distribution between conformers A and B. The lack of A H-2/B H-5 and B H-2/C H-5 NOEs and the presence of A H-1/B H-5 and B H-2/C H-5 NOEs with medium-size intensities indicates that, for the *V. cholerae* oligosaccharides, conformer B is indeed present in the conformational equilibrium with an important participation, in contrast with the reports for the *Brucella* O-polysaccharides, for which conformer A was deduced to be predominant [24]. Nevertheless, the steric energy difference between A and B is indeed small, according to the MM3* calculations, and both conformers are predicted to exist.

The results obtained indicate that these unrestrained MD simulations [26] provide a fair description of the motion around the different glycosidic linkages of this molecule, at least in this particular case. Regarding the acyl chain, there are no NOE contacts between its protons and those of the oligosaccharide, apart from the trivial ones with the corresponding H-4, indicating that this chain may adopt a variety of conformations. Nevertheless, the coupling constants for the β protons are ca. 3.9 and 8.5 Hz, similar to those reported for the monosaccharide entities, indicating a favored orientation around the β–γ linkage. These values are in good agreement with those expected for the calculations described above and with the X-ray data [21,22].

Summarizing the theoretical results, the terminal methyl group has, therefore, no effect on the conformation of the Ogawa O-PS. It seems that there is a reasonable amount of conformation freedom for the glycosidic and exocyclic torsion angles of both trisaccharides, although a representative major conformer may be deduced from Fig. 4. It seems reasonable to think from the data obtained herein that the nature of the receptor binding sites may modulate the biological response of both antigens, through different van der Waals and/or hydrogen bond interactions with the two antigens. In fact, recent binding studies [6] of derivatives of the Ogawa monosaccharide and two antibodies have shown that the C-2 O-methyl group fits into a cavity of the antibody and that hydrogen bonds involving the 2

and 3 positions of the sugar moiety as well as the β position in the amide side chain are required.

Acknowledgements

Financial support from the DGICYT (Grant PB96-0833) is gratefully acknowledged. L.G. and J.L.A. thank the Ministerio de Educacion y Ciencia and CAM for postdoctoral fellowships. We thank one of the referees for bringing to our attention the previous work of Professor Bundle.

References

[1] A.V. Barlett, *Lancet*, 338 (1991) 1216.
[2] N.W. Preston, *Lancet*, 342 (1993) 925–926.
[3] (a) J.W. Redmond, *Biochim. Biophys. Acta*, 584 (1979) 346–352. (b) T. Ito, T. Higuchi, M. Hirobe, K. Hiramitsu, T. Yokota, *Carbohydr. Res.*, 256 (1994) 113–128.
[4] K. Hisatsune, S. Kondo, Y.S Isshiki, Y. Iguchi, Y. Haishima, *Biochem. Biophys. Res. Commun.*, 190 (1993) 302–307.
[5] A. Arencibia-Mohar, O. Madrazo-Alonso, A. Ariosa-Alvarez, J. Sarracent-Perez, M. Alfonso, J.L. Perez, M. Ramirez, R. Montes, V. Verez-Bencomo, *Carbohydr. Lett.*, 1 (1995) 173–178.
[6] J. Wang, S. Villeneuve, J. Zhang, P. Lei, C.E. Miller, P. Lafaye, F. Nato, S.C. Szu, A. Karpas, S. Bystricky, J.B. Robbins, P. Kovac, J.M. Fournier, C.P. Glaudemans, *J. Biol. Chem.*, 273 (1998) 2777–2783.
[7] S. Kondo, Y. Sano, Y. Isshiki, K. Hisatsune, *Microbiology*, 142 (1996) 2879–2885.
[8] D.R. Bundle, H. Baumann, J.-R. Brisson, S.M. Gagne, A. Zdanov, M. Cygler, *Biochemistry*, 33 (1994) 5183–5190.
[9] A. Poveda, J. Jimenez-Barbero, *Chem. Soc. Rev.*, 27 (1998) 133–143.
[10] For the synthesis of different fragments, see: (a) Y. Ogawa, P.A. Kovac, *Glycoconjugate J.* 14 (1997) 433–438 and Refs. therein. (b) A. Arencibia-Mohar, A. Ariosa-Alvarez, O. Madrazo-Alonso, E. Gonzalez Abreu, L. Garcia-Imia, G. Sierra-Gonzalez, V. Verez-Bencomo, *Carbohydr. Res.*, 306 (1998) 163–170.
[11] N.L Allinger, Y.H. Yuh, J.H. Lii, *J. Am. Chem. Soc.*, 111 (1989) 8551–8557.
[12] F. Mohamadi, N.G.I. Richards, W.C. Guida, R. Liskamp, C. Canfield, G. Chang, T. Hendrickson, W.C. Still, *J. Comput. Chem.*, 11 (1990) 440–467.
[13] (a) A.D. French, J.D. Brady (Eds.), *Computer Modelling of Carbohydrate Molecules*, ACS Symp. Ser., 1990. (b) M.K Dowd, J. Zeng, A.D. French, P.J. Reilly, *Carbohydr. Res.*, 247 (1992) 51–62.
[14] (a) S.W. Homans, *Biochemistry*, 29 (1990) 9110–9118. (b) B.J. Hardy, W. Egan, G. Widmalm, *Int. J. Biol. Macromol.*, 17–18 (1995) 149–160. (c) C.J. Edge, U.C. Singh, R. Bazzo, G.L. Taylor, R.A. Dwek, T.W. Rademacher, *Biochemistry*, 29 (1990) 1971–1974. (d) P.J. Hajduk, D.A. Horita, L. Lerner, *J. Am. Chem. Soc.*, 115 (1993) 9196–9201. (e) T.J. Rutherford, D.G. Spackman, P.J. Simpson, S.W. Homans, *Glycobiology*, 4, (1994) 59–68. (f) A. Poveda, J.L. Asensio, M. Martin-Pastor, J. Jimenez-Barbero, *J. Chem. Soc., Chem. Commun.*, (1996) 421–422.
[15] W.C. Still, A. Tempczyk, R.C. Hawley, T. Hendrickson, *J. Am. Chem. Soc.*, 112 (1990) 6127–6128.
[16] J.L. Asensio, M. Martin-Pastor, J. Jimenez-Barbero, *Int. J. Biol. Macromol.*, 17 (1995) 52–55.
[17] (a) J.L. Asensio, M. Martin-Pastor, J. Jimenez-Barbero, *J. Mol. Struct. (Theochem)*, 395–396 (1997) 245–265. (b) M. Martin-Pastor, J.L. Asensio, R. Lopez, J. Jimenez-Barbero, *J. Chem. Soc., Perkin Trans 2*, (1995) 713–721. (c) I. Robina, E. López-Barba, J. Jiménez-Barbero, M. Martín-Pastor, J. Fuentes, *Tetrahedron: Asymmetry*, 8 (1997) 1207–1224. (d) A. Poveda, C. Vicent, S. Penadés, J. Jimenez-Barbero, *Carbohydr. Res.*, 301 (1997) 5–10. (e) A. Poveda, M. Santamaría, M. Bernabe, A. Prieto, M. Bruix, J. Corzo, J. Jimenez-Barbero, *Carbohydr. Res.*, 304 (1997) 209–217.
[18] R.U. Lemieux, K. Bock, L.T.J. Delbaere, S. Koto, V.S. Rao, *Can. J. Chem.*, 58 (1980) 631–653.
[19] D. Neuhaus, M.P. Williamson, *The Nuclear Overhauser Effect in Structural and Conformational Analysis*, VCH, New York, 1989.
[20] K. Bock, J. Duus, *J. Carbohydr. Chem.*, 13 (1994) 513–543.
[21] M. Gotoh, C.N. Barnes, P. Kovac, *Carbohydr. Res.*, 260 (1994) 203–218.
[22] P. Lei, Y. Ogawa, J.L. Flippen-Anderson, P. Kovác, *Carbohydr. Res*, 279 (1995) 117–129.
[23] (a) K. Bock, *Pure Appl. Chem.*, 55 (1983) 605–622. (b) J.P. Carver, *Pure Appl. Chem.*, 65 (1993) 763–770 (c) D.A. Cumming, J.P. Carver, *Biochemistry*, 26 (1987) 6664–6676.
[24] (a) T. Peters, D. Bundle, *Can. J. Chem.*, 68 (1990) 979–988. (b) D. Bundle, J.W. Cherwonogrodzky, M.B. Perry, *Biochemistry*, 26 (1987) 8717–8726 (c) J. Kihlberg, D. Bundle, *Carbohydr. Res.*, 216 (1991) 67–78.
[25] M. Caroff, D.R. Bundle, M.B. Perry, J.W. Cherwonogrodzky, J.R. Duncan, Infect, *Immunol.*, 46 (1984) 384–388.
[26] (a) T.J. Rutherford, S.W. Homans, *Biochemistry*, 33 (1994) 9606–9614. (b) T.J. Rutherford, D.C.A. Neville, S.W. Homans, *Biochemistry*, 34 (1995) 14131–14137.